AMERICAN ACADEMY OF OPHTHALMOLOGY®

Retinal Vascular Permeability in Diabetic Subjects without Retinopathy Compared with Mild Diabetic Retinopathy and Healthy Controls

Sarah R. Vavrek,[1] Elif Kayaalp Nalbant, PhD,[1] Nicholas Konopek,[2] Nicole L. Decker,[2] Amani A. Fawzi, MD,[2] William F. Mieler, MD,[3] Kenneth M. Tichauer, PhD,[1] Jennifer J. Kang-Mieler, PhD[4]

Objective: To investigate retinal vascular permeability mapping as a potential biomarker for diabetic retinopathy in subjects with diabetes with no signs of retinopathy and with mild nonproliferative retinopathy.

Design: This is a case-control study.

Subjects: Participants included 7 healthy controls, 22 subjects with diabetes mellitus and no clinical signs of retinopathy (DMnoDR), and 7 subjects with mild nonproliferative diabetic retinopathy (NPDR).

Methods: All participants underwent routine retinal fluorescein videoangiography (FVA). Each FVA dataset was analyzed with the dynamic tracer kinetic model (DTKM) method to estimate 5 parameters: extraction fraction (*E*), blood flow, arrival time, transit time, and rate constant defined via adiabatic solution. The DTKM method was based on indicator dilution theory, including sequential use of 2 prominent kinetic models: the plug flow model and the adiabatic approximation to the tissue homogeneity model.

Main Outcome Measures: Extraction fraction, i.e., the fluorescein dye leakage measured during 1 pass through surrounding retinal tissue, is extracted via DTKM method and directly relates to retinal vascular permeability. Thus, *E* represents the preclinical biomarker, retinal vascular permeability.

Results: The 3 diagnostic groups were found to have significantly different permeability ($P = 0.003$). Despite having no clinical signs of retinopathy, the mean rank of average vascular *E* was significantly higher in DMnoDR subjects compared with healthy controls ($P = 0.04$), as was the mean rank of *E* for mild NPDR subjects ($P = 0.002$). The average *E* for mild NPDR, DMnoDR, and control subjects was 0.10 ± 0.04, 0.07 ± 0.04, and 0.04 ± 0.01, respectively.

Conclusions: The vascular permeability extracted from FVA datasets using the DTKM method is a promising biomarker for detecting preclinical retinal pathology in patients with diabetes. Longitudinal studies are ongoing to explore the ability of this biomarker to distinguish those subjects with diabetes who will progress to clinically apparent retinopathy from those who will not.

Financial Disclosure(s): Proprietary or commercial disclosure may be found in the Footnotes and Disclosures at the end of this article. *Ophthalmology Science 2025;5:100636 © 2024 by the American Academy of Ophthalmology. This is an open access article under the CC BY-NC-ND license (http://creativecommons.org/licenses/by-nc-nd/4.0/).*

Up to 90% of vision impairment and loss linked to diabetes mellitus could be prevented with earlier detection than is possible with current clinical diagnostics.[1] Preclinical biomarker development is critical in the mitigation of diabetic-related vision loss. Measurement of physiological parameters associated with retinal microvascular abnormalities, e.g., retinal vascular permeability, have been proposed as potential early biomarkers for diabetic retinopathy (DR).[2] Currently, there are no clinically established approaches to quantitatively analyze retinal vascular permeability.[3]

Healthy retinal microvasculature is tightly regulated through the blood-retinal barrier. Disruptions to the blood-retinal barrier (e.g., pericyte dropout, interendothelial tight junction loss, and basement membrane thickening) are hallmark characterizations that occur in the early stages of DR and lead to increased retinal vascular permeability.[4–6] The current gold standard for determining changes in permeability in preclinical animal models requires injection of an Evans Blue (or similar) dye. The retinal vascular permeability is then estimated from ex vivo retina (post-euthanasia) by comparing the amount of dye that has extravasated among different tissues, making this approach unsuitable for clinical translation.[7] Alternative noninvasive approaches (e.g., extracting permeability via dual tracer fluorescein angiographies; and extracting permeability via spectral OCT) have been tested on animal models but have not been successfully translated to the clinic.[8–14] Rapid eye motion and resolution requirements make currently available methods that noninvasively measure

https://doi.org/10.1016/j.xops.2024.100636
ISSN 2666-9145/24

permeability in other areas of the body of little utility for retinal applications (e.g., magnetic resonance imaging and dynamic contrast enhanced computed tomography).[15–18] OCT angiography and adaptive optics scanning laser ophthalmoscopy have shown some promise for detecting early structural changes in the retinal vasculature.[19–21]

The objective of this work is to showcase that an indicator-dilution method applied to a routine retinal fluorescein videoangiography (FVA) dataset can be utilized to quantify vascular permeability—a functional parameter of the vasculature that is hypothesized to be affected prior to the early structural changes detectable by OCT angiography and adaptive optics scanning laser ophthalmoscopy—in the retinas of human subjects.[22–24] Established in the 1950s, Meier and Zierler's indicator-dilution method has been used to quantify blood flow from the dynamics of a contrast agent measured in the blood and tissue.[25] The adiabatic approximation to the tissue homogeneity (AATH) model,[26] an adaptation of the Johnson & Wilson model,[27] was developed by St. Lawrence and Lee in 1998, enabling the estimation of both blood flow and vascular permeability. More recently, these methods have been modified by our group for retinal FVA analysis in rat models and demonstrated feasibility while enabling flexibility in fluorescein tissue arrival time.[28,29] Although blood flow estimates are extracted and monitored, our main objective in this work is to estimate vascular permeability. This work presents the first adaptation of our methods to human subjects as part of a 5-year longitudinal study monitoring vascular permeability in patients with diabetes mellitus without DR (DMnoDR), as well as those with mild, moderate, and severe nonproliferative DR (NPDR). We compare the findings to those in healthy controls without diabetes mellitus and ultimately plan to correlate changes in retinopathy over time and vision loss with vascular permeability. This study presents the demonstration of feasibility and baseline findings in 22 DMnoDR subjects, 7 mild NPDR subjects, and 7 healthy control subjects.

Methods

Subject Information

All procedures were carried out with approval from Institutional Review Boards at Northwestern University and the University of Illinois Chicago, who reviewed clinical procedures based on the principles embodied in the Declaration of Helsinki. The study was conducted at the Department of Ophthalmology and Visual Sciences at the University of Illinois Chicago and the Department of Ophthalmology at Northwestern University, with the understanding and written consent of each subject. Seven subjects with mild NPDR, 22 subjects with DMnoDR, and 7 healthy control subjects were included in this study. General demographic information and body mass index (BMI) were collected from all 3 groups at the time of FVA data collection (Table 1). The DMnoDR and mild NPDR subjects' age of diagnosis, diabetes type, percent hemoglobin A1c, mean arterial pressure, and intraocular pressure (IOP) of the eye imaged were also obtained (Table 1).

Table 1. General Subject Information

Subject Information	Healthy Controls (n = 7)	DMnoDR (n = 22)	Mild NPDR* (n = 7)
Demographics			
Age at data collection (yrs)	40 ± 10	50 ± 10	60 ± 10
Age at diagnosis (yrs)	NA	40 ± 10 (n = 19)	60 ± 10
Duration of diagnosis (yrs)	NA	11 ± 9 (n = 19)	6 ± 7
Male/female	4/3	10/12	2/5
Type 1/type 2 diabetes	0/0	4/18	0/7
OD/OS study eye	4/3	21/1	6/1
Race			
Native Hawaiian/Pacific Islander	0	1	0
White	3	9	4
Black	2	6	1
Asian	1	2	0
Multiracial	0	1	0
Other	1	2	0
Declined	0	1	1
Ethnicity			
Non-Hispanic	6	17	3
Hispanic	1	5	3
Declined	0	0	1
Subject assessment			
BMI (kg/m^2)	29 ± 8	33 ± 7	34 ± 8
HbA1c (%)	NA	7 ± 1	6.2 ± 0.6
Mean arterial pressure (mmHg)	NA	100 ± 10	90 ± 10
IOP of study eye (mmHg)	NA	16 ± 2 (n = 21)	16 ± 3

BMI = body mass index; DMnoDR = diabetes mellitus no diabetic retinopathy; HbA1c = hemoglobin A1c; IOP = intraocular pressure; NPDR = nonproliferative diabetic retinopathy; OD = right eye; OS = left eye.
*Six of the 7 mild NPDR subjects' races were available.

Data Collection Procedure

Each retinal FVA was taken using a scanning laser ophthalmoscope (SLO) (SPECTRALIS Heidelberg Retina Angiography + OCT, Heidelberg Engineering Inc). All the control FVAs, 21 of the DMnoDR FVAs, and 6 of the mild NPDR FVAs were taken at "High Speed." The 22nd DMnoDR FVA and seventh mild NPDR FVA were taken at "High Resolution." (Note: the collection mode does not affect the results of model fitting to data; results not shown). A 55° widefield lens was used for all data collection. The SLO's sensitivity was set at 74%, and frames inadvertently not collected at 74% were scaled appropriately based on a gain-to-signal calibration factor.[30] An intravenous bolus injection of 0.5 ml of 10% fluorescein (Fluorescite) was administered and immediately followed by a ~2-ml bolus of saline. The SLO's fluorescein angiography timer was simultaneously initiated at the start of the injection. Each FVA was taken for a duration of ~2 minutes.

Pre-Dynamic Tracer Kinetic Model Procedure for Fluorescein Videoangiographies

All the DMnoDR and mild NPDR FVAs and 5 of the control FVAs were exported as uncompressed 24-bit Audio Video Interleaves (AVIs) with the "Unsmoothed Pixels" option. The 24-bit AVIs have three 8-bit channels holding the same data; thus, only a single 8-bit channel is truly available. Frames that contained blinking, shadowing, or any defect (e.g., in rare cases, sections of frames or whole frames were composed of Gaussian noise) were removed using an in-house semiautomated frame removal software written in MATLAB (MathWorks), which has been described in detail elsewhere.[30]

The 8-bit AVI with no poor-quality frames then underwent motion correction with the use of the commercial software, Dynamic ICG (Lickenbrock Technology).[31] At least 5 preinjection frames (frames just before fluorescein enhancement) were initially kept for background subtraction. Any excess preinjection frames were cropped prior to motion correction. Software options selected for all datasets included: "Nearest Slice" alignment method, "inter-movie Laplacian," "black" void region fill, "no interpolation," "automatic" base channel, and "very severe" image warping. Settings were selected based on a trial-and-error-based qualitative analyses of motion correction results across the cohort of AVIs.

Postmotion correction, frames that did not align well with the overall video (observed as spatial shifts in the large blood vessels) were manually removed. The usable frames (spanning 20−90 s) had background (preinjection) signal subtracted. A single preinjection frame (frame just before fluorescein enhancement) was subtracted from all subsequent frames for a background signal (e.g., autofluorescence) removal. The frames were subsequently checked for oversaturated pixels; any pixel ≥90% of the saturation level of the SLO was considered oversaturated and ignored (owing to known nonlinearities in signal near saturation).

Dynamic Tracer Kinetic Model Procedure

The dynamic tracer kinetic model (DTKM) theory is based on established kinetic modeling methods (Fig. 1A[25,26]) and has been described in detail and evaluated to estimate retinal vascular permeability in animal models.[28] Briefly, the approach entails using nonlinear least-squares curve fitting using equations (1) and (2) to estimate various hemodynamic and vascular parameters from measured fluorescein signals over time extracted from retinal tissue and a retinal artery. The mathematical representation of fluorescein signal in retinal tissue, $S_{tis}(t)$, as a function of time, t, can be represented as:

$$S_{tis}(t) = FS_a(t) * R(t) \quad (1)$$

where $S_a(t)$ represents the measured fluorescein signal in a retinal artery, F represents the blood flow, and $R(t)$ represents the "impulse residue function," which can be further represented as:

$$R(t) = \begin{cases} 0, t < t_a \\ 1, t_a \le t \le t_a + t_\tau \\ Ee^{-k_{adb}(t-t_a-t_\tau)}, t > t_a + t_\tau \end{cases} \quad (2)$$

where t_a represents the "arrival time," i.e., time it takes for the fluorescein to transit from the location of the $S_a(t)$ measurement site to the $S_{tis}(t)$ measurement site; t_τ represents the "tissue transit time," which is equivalent to the ratio of the blood volume to the blood flow; k_{adb} is the "adiabatic rate constant," which is proportional to the likelihood fluorescein will diffuse from the tissue to the blood; and E represents the "extraction fraction", equivalent to the fraction of fluorescein that "leaks" from blood to tissue on a single pass of blood volume. Since E is directly related to vascular permeability, it is the main parameter of interest in this work.

Retinal arterial signals, $S_a(t)$, were collected by taking the average preprocessed FVA signal as a function of time from a

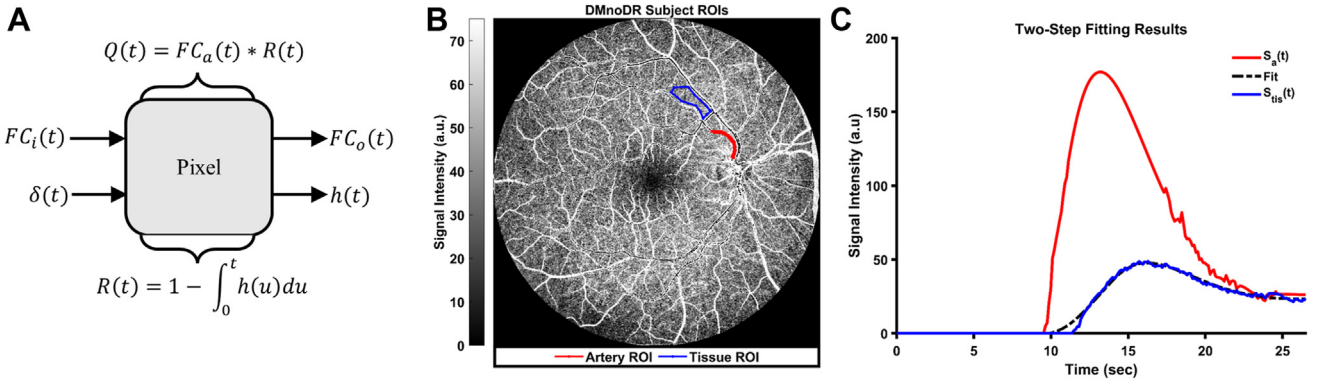

Figure 1. Dynamic tracer kinetic model (DTKM) theory. **A,** The singular pixel represents retinal tissue as a linear time-invariant system. Parameters include blood flow (F), input concentration function ($C_i[t]$), unit impulse function ($\delta[t]$), output concentration function ($C_o[t]$), impulse response function ($h[t]$), tissue fluorescein concentration function ($Q[t]$), and impulse residue function ($R[t]$).[24,25] **B,** An example diabetic subject without retinopathy's (DMnoDR) fluorescein uptake image at peak signal includes arterial (red) and tissue (blue) regions of interest (ROIs). **C,** The corresponding arterial signal ($S_a[t]$), tissue signal ($S_{tis}[t]$), and nonlinear least-squares fitting results using the DTKM (dashed line) are presented.

region of interest (ROI) manually drawn on a large artery (e.g., Fig 1B). Retinal tissue signals, $S_{tis}(t)$, were collected from preprocessed FVAs in 2 ways: (1) by manually drawing ROIs on the retinal tissue (3 ROIs averaged from each FVA; e.g., Fig 1B) and (2) in a pixel-by-pixel fashion (treating each 2x2 pixel bin as an $S_{tis}[t]$).

Nonlinear least squares curve fitting using fminsearch in MATLAB was then carried out on all $S_{tis}(t)$s to approximate the 5 fitting parameters: F, t_a, t_τ, k_{adb}, and E. To minimize variance in the parameter estimations, the fitting was carried out in 2 steps: F, t_a, and t_τ were first approximated by setting $E = 0$ and fitting up to the $S_{tis}(t)$ peak,[29] then a 5-parameter fit was applied to the whole curve while constraining F, t_a, and t_τ estimates to within 10% of their approximated values.[28]

Statistical Analysis

MATLAB was used to test normality and complete all parametric and nonparametric tests. Shapiro-Wilk testing was conducted to test the normality. Parametric analyses were used when all data passed the normality test; nonparametric analyses were used otherwise. For parametric and nonparametric correlations, 2-tailed Pearson and Spearman correlation tests were used, respectively. For parametric and nonparametric grouped analysis, 1-way or multi-way analysis of variance (ANOVA) and Kruskal-Wallis tests were used, respectively. Upon completion of 1-way ANOVA and Kruskal-Wallis tests, Tukey-Kramer's Honestly Significant Difference test was conducted on both parametric and nonparametric data. Analysis of all subjects as well as age-matched subjects was conducted.

Results

Subject information, including demographic (i.e., age at data collection, age at diagnosis, duration of disease, disease, gender, race, and ethnicity) and baseline clinical characteristics (i.e., BMI, hemoglobin A1c, mean arterial pressure, and IOP of study eye) are included in Table 1. The Shapiro-Wilk test showed that the control's k_{adb}, DMnoDR's E, F, t_a, k_{adb}, permeability-surface area product (PS), and duration of diagnosis, and mild NPDR's PS, age at diagnosis, and duration of diagnosis did not have normal distribution and therefore are nonparametric; all other group factors were found to be parametric. Based on a 2-tailed t-test between DMnoDR and control subjects' average tissue ROIs at peak fluorescence, there were no clinically observable statistically significant differences. No statistical significance was found between the BMI between control subjects, DMnoDR subjects, and mild NPDR subjects using the 2-tailed Kruskal-Wallis test. There was a statistically significant difference ($P = 0.007$) between the age at data collection between the 3 diagnostic groups using 1-way ANOVA. Based on Tukey-Kramer's Honestly Significant Difference testing, there was no statistically significant difference between the mean ranks of age at data collection between control and DMnoDR subjects or DMnoDR and mild NPDR subjects; however, the mean age at data collection between control and mild NPDR subjects was found to be significantly different ($P = 0.005$). Therefore, analysis of all DMnoDR and mild NPDR subjects and analysis of DMnoDR and mild NPDR subjects age-matched with the control group was conducted.

DTKM Outputs

The 2-step model fitting yielded a final estimation of F, t_a, t_τ, E, and k_{adb} using a modified AATH model[29] on the control, DMnoDR, and mild NPDR datasets, and PS was calculated using E and F estimations. Mean and standard deviation of all parameters for all control, DMnoDR, and mild NPDR subjects were calculated, as were the mean and standard deviation of all parameters for the DMnoDR and mild NPDR subjects age-matched to the control group (Table 2). Vascular permeability—as represented by E—result comparisons between control, DMnoDR, and mild NPDR groups are presented in Fig 2A. Extraction fraction was mapped pixel-by-pixel for each dataset; a comparison of examples of healthy control, DMnoDR, and mild NPDR datasets are provided (Fig 2B–G).

A significant difference in E between all DMnoDR, mild NPDR, and healthy control subjects was determined ($P = 0.003$), with DMnoDR and mild NPDR having significantly higher mean Es than the control group ($P = 0.04$ and $P = 0.002$, respectively). No other AATH fitting parameters were observed to yield statistically significant differences between the 3 diagnostic groups. A statistically significant difference in E was found between the 3 age-matched diagnostic groups using 1-way ANOVA ($P = 0.02$). The means of control and mild NPDR groups were found to be significantly different, with mild NPDR group's mean E

Table 2. DTKM-Extracted Parameters

DTKM-Extracted Parameters	E (Unitless)	F* (ml·100g^{-1}·min^{-1})	t_a (s)	t_τ (s)	k_{adb} (min^{-1})	PS* (ml·100g^{-1}·min^{-1})
All subjects						
Healthy controls	0.04 ± 0.01	500 ± 300	0.7 ± 0.5	4 ± 2	0.003 ± 0.004	17 ± 7
DMnoDR	0.07 ± 0.04	400 ± 200	0.7 ± 0.6	4 ± 1	0.004 ± 0.004	35 ± 36
Mild NPDR	0.10 ± 0.04	400 ± 200	0.4 ± 0.2	4 ± 1	0.004 ± 0.003	47 ± 42
Age-matched subjects						
DMnoDR	0.07 ± 0.05	400 ± 200	0.7 ± 0.6	4 ± 1	0.003 ± 0.004	36 ± 37
Mild NPDR	0.11 ± 0.05	400 ± 300	0.3 ± 0.2	5 ± 1	0.005 ± 0.002	56 ± 56

DTKM = dynamic tracer kinetic model; DMnoDR = diabetes mellitus no diabetic retinopathy; NPDR = nonproliferative diabetic retinopathy; E = extraction fraction; F = blood flow; t_a = arrival time; t_τ = transit time; k_{adb} = rate constant defined by adiabatic solution; PS = permeability-surface area product.
*F and PS are measured as ml·100g^{-1}·min^{-1}, where the unit term, 100 g, refers to 100 g of retinal tissue.

higher than the control group's mean E ($P = 0.02$), and the means between control and DMnoDR groups were found to be nearing statistically significantly different, with DMnoDR group's mean E higher than the control group's mean E ($P = 0.1$). No other DTKM-extracted parameter was statistically significant in the age-matched comparison.

Correlation of Fitting Parameters with Patient Physiological Parameters

Extraction fraction was compared with control, DMnoDR, and mild NPDR subjects' age at data collection and BMI, as well as with DMnoDR and mild NPDR subjects' age of diagnosis, duration of diagnosis, hemoglobin A1c, mean arterial pressure, and imaged eye's IOP (Fig 3). No statistically significant correlations were observed between any fitting parameter and any of the patient physiology parameters.

Discussion

The intention of this study was to demonstrate the ability to estimate and map retinal vascular permeability in healthy control subjects, DMnoDR subjects, and mild NPDR subjects using a 2-step nonlinear least squares fitting of a kinetic model to retinal FVA data. This is the initial step of a 5-year-long study where retinal vascular permeability

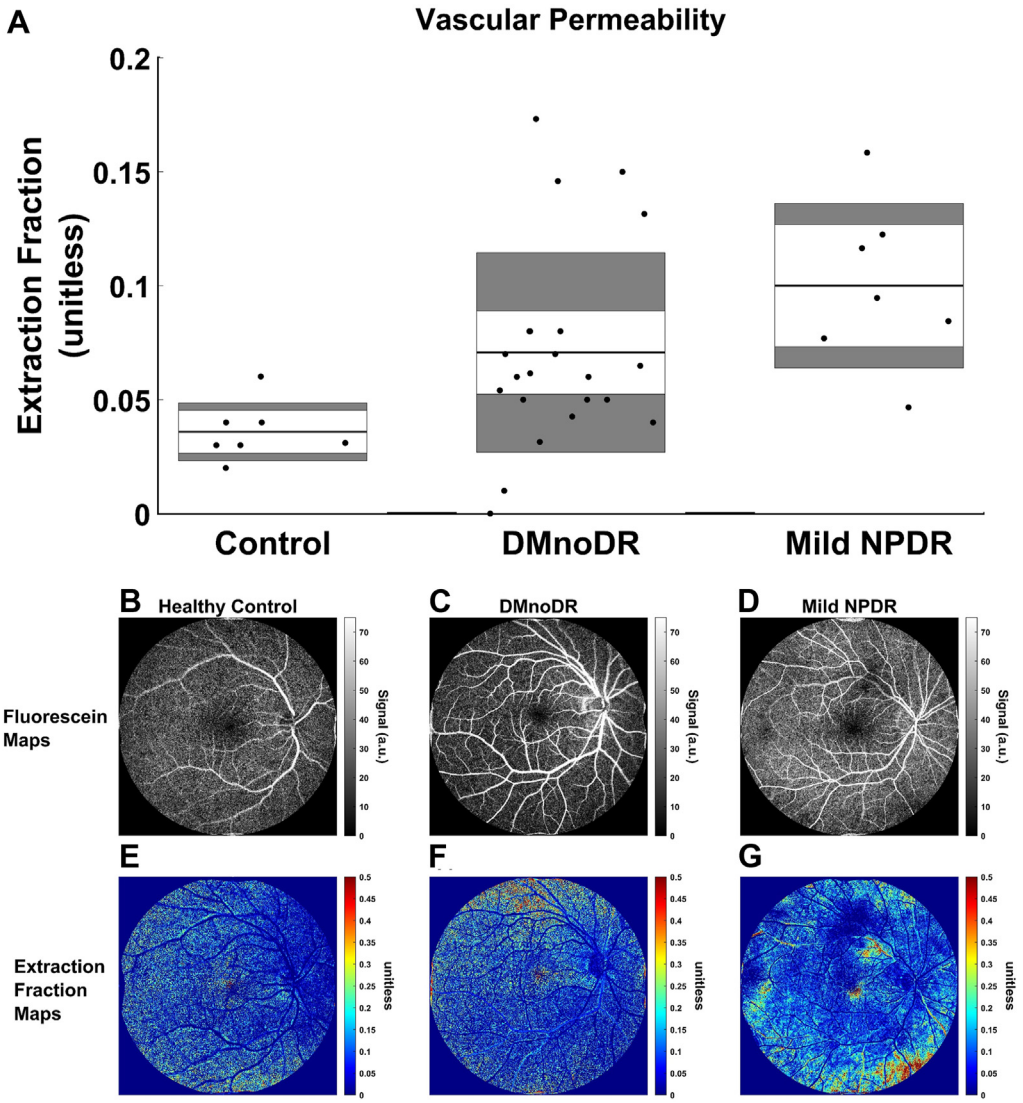

Figure 2. Retinal vascular permeability in healthy control, DMnoDR, and mild NPDR subjects. **A,** Modified boxplots[32] of extraction fraction collected for healthy control subjects, DMnoDR subjects, and mild NPDR subjects. Modified boxplots use mean and standard errors of the mean in place of median and standard deviation, respectively. A 95% confidence interval of the mean is also used. Examples of pixel-by-pixel fluorescein maps for (**B**) control, (**C**) DMnoDR, and (**D**) mild NPDR subjects. The extraction fraction maps for (**E**) healthy control, (**F**) DMnoDR, and (**G**) mild NPDR subjects have unitless units that are fractional units from 0 to 1. DMnoDR = diabetes mellitus no diabetic retinopathy; NPDR = nonproliferative diabetic retinopathy.

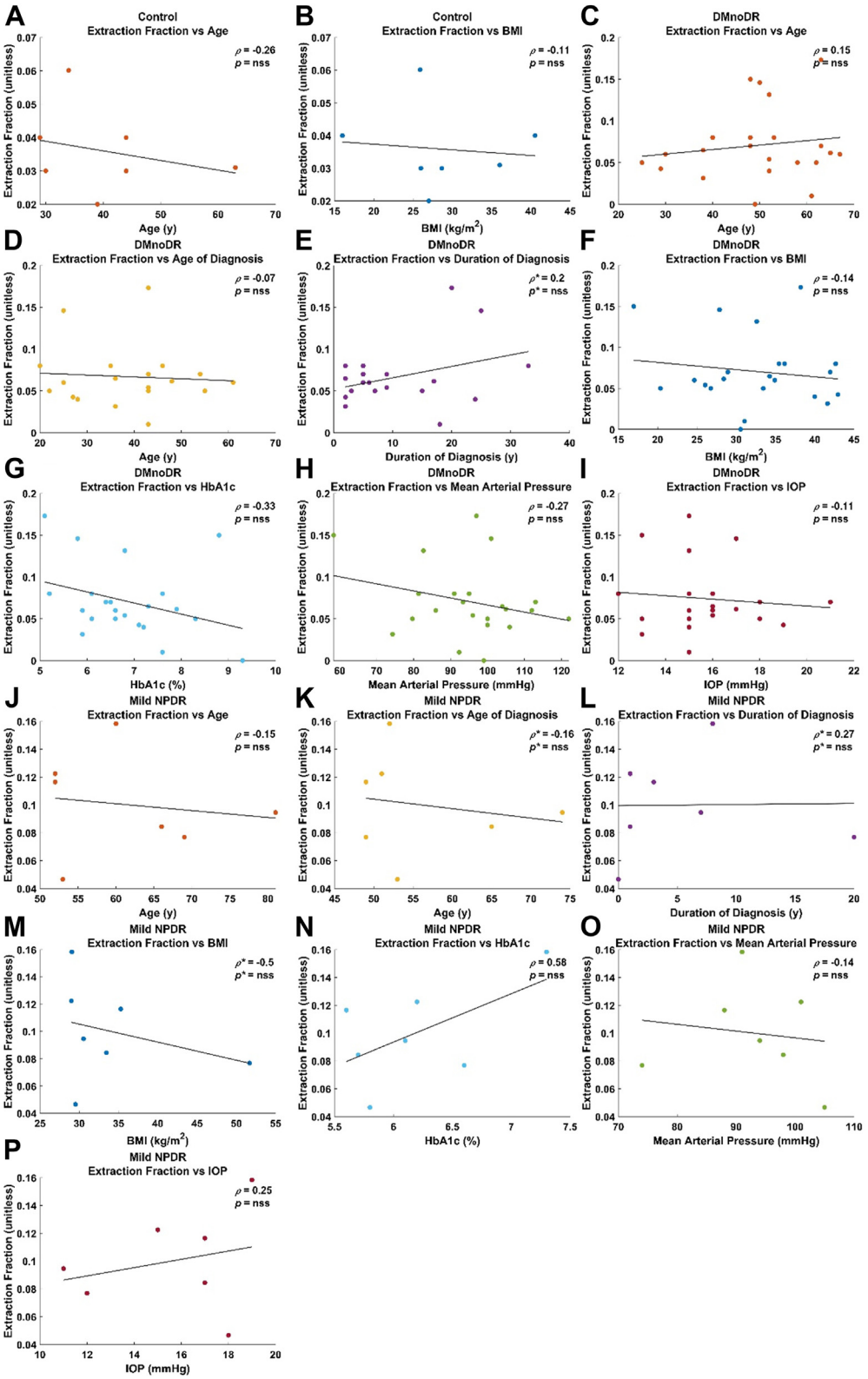

Figure 3. Correlation of extraction fraction vs. healthy control, DMnoDR, and mild NPDR subject information. Correlation plots of extraction fraction vs. **(A)** age at data collection, and **(B)** BMI for healthy control subjects; **(C-I)** and **(J-P)** are of extraction fraction vs. the age at data collection, age of diagnosis, duration of diagnosis, BMI, HbA1c, mean arterial pressure, and IOP, of the eye imaged for DMnoDR and mild NPDR subjects, respectively. The resulting correlation coefficient (ρ) and *P*-value (*p*) with * indicates Spearmen tests; ρ and *p* without * indicates Pearson testing; and nss is not statistically significant. BMI = body mass index; DMnoDR = diabetes mellitus no diabetic retinopathy; HbA1c = hemoglobin A1c; IOP = intraocular pressure; NPDR = nonproliferative diabetic retinopathy.

measured in DMnoDR and mild NPDR subjects is being tracked and compared with all observed clinical markers of diabetic retinopathy as well as with control subjects. The primary findings indicated that despite the diabetic subjects having no clinical signs of retinal abnormalities, their vascular permeability—estimated through E—was significantly higher when compared to the healthy controls, as was the E of subjects with mild NPDR subjects. No statistical significance was found between DMnoDR and mild NPDR subjects.

There are currently no alternative clinical methods that allow direct estimation of retinal vascular permeability.[21] Current established methods that are available either require invasive techniques or do not have the spatial resolution necessary to evaluate the retina (retinas are <0.3 mm thick[33]).[15,16] This makes it impossible to directly validate the vascular permeability values estimated in this work. Previous studies have used posterior vitreous fluorophotometry to assess blood-retinal barrier breakdown in patients with diabetes and either no DR, minimal DR, or both no and minimal DR, with mixed results that are difficult to compare because of the reliance on different techniques and fluorophotometers.[34–38] Chahal et al did not find any significant difference between the permeability coefficient (p), diffusion coefficient (D), or permeability index (PI) in insulin-dependent diabetic patients with no or minimal DR ($p = 1.94 \pm 1.03$ cm·s^{-1}·10^{-7}; $D = 1.74 \pm 1.53$ cm^2 s^{-1}·10^{-5}; $PI = 2.14 \pm 1.21$ cm·s^{-1}·10^{-7}) and healthy control subjects ($p = 1.99 \pm 0.95$ cm·s^{-1}·10^{-7}; $D = 2.05 \pm 1.03$ cm^2·s^{-1}·10^{-5}; $PI = 1.15 \pm 0.38$ cm·s^{-1}·10^{-7}), whereas in a comparable study conducted by Cunha-Vaz et al, the posterior vitreous fluorescein concentration and penetration ratio (i.e., ratio between posterior vitreous fluorescein concentration and free plasma fluorescein concentration) in diabetic patients with no or 1 aneurysm were both significantly higher compared with healthy control patients.[36,37] In a dual tracer study conducted on healthy Long Evans rats, the vascular permeability as represented by E was 0.08 at baseline (n = 13) and 0.15 post-mannitol infusion (n = 3),[10] which is significantly higher than the observed Es in this human study (0.04 ± 0.01, 0.07 ± 0.04, and 0.10 ± 0.04 for control, DMnoDR, and mild NPDR groups, respectively). Both E and k_{adb} (parameters estimated in this work) are related to vascular permeability, which is often reported as the permeability-surface-area-product, PS. However, we are focusing on E in this work because the precision of its estimation is less sensitive to noise than k_{adb}.[28] Note: injection-site-to-retina time and injection site location have no effect on the DTKM-extracted parameters because the DTKM uses arterial signals collected from the retina as an input function, providing an internal control for dose and site of injection. Other microvasculature characteristics outside of retinal vascular permeability have also been assessed; a meta-analysis evaluating control versus DMnoDR microvasculature changes using OCT angiography found decreases in radial pericapillary capillary perfusion density and macular perfusion density (excluding fovea) and increases in perimeter and area of the foveal avascular zone in the DMnoDR microvasculature.[21]

It should be noted that while the ages of the DMnoDR group and the control group were not different to a statistically significant degree, the control group was younger than the mild NPDR group. However, correlations suggested that age does not have any significant effect on the differences observed in E between groups (Fig 3), as there was no correlation between age and vascular parameters within any group. Moreover, a statistical comparison of the subset of DMnoDR and mild NPDR patients that were age-matched with the controls yielded similar statistical differences as the full dataset comparisons.

Previous studies found blood flow, F, to be 3.09 ml·100 g^{-1}·min^{-1} (9.52 µl·min^{-1}), 4 ± 1.1 ml·100 g^{-1}·min^{-1} (13 ± 3.2 µl·min^{-1}), and 26 ± 4 ml·100 g^{-1}·min^{-1} (80 ± 20 µl·min^{-1}) in healthy human subjects, 2.96 ml·100 g^{-1}·min^{1} (9.12 µl·min^{-1}) in DMnoDR subjects, and 19.8 ± 12.4 ml·100 g^{-1}·min^{-1} in cats under normal conditions.[39–42] In this work, 10 to 20 times higher blood flows were estimated. It is most likely that a higher level of attenuation of fluorescein fluorescence light in blood compared to tissue is most likely the cause.[43–45] Blood attenuation is expected to be 2 to 3 orders-of-magnitude higher than tissue attenuation, which, even over a 0.3 mm retinal thickness, is likely to lead to significant underestimations in large vessel fluorescein signal detection.[46] Despite overestimations in blood flow, it is likely that such attenuation effects are consistent between the study groups, so differences in blood flow between groups could be relevant, and the blood flow error is linked only to a scaling factor error and will not have any significant effect on the estimates of E, the main parameter of interest in this work.

The significant differences in E between groups were seen in relatively randomly selected regions of the retina that avoided large blood vessels; however, all fitting parameters were also estimated on a "pixel-by-pixel" basis, providing parametric maps that may provide a much richer dataset for detection and diagnosis of retinal vascular and hemodynamic abnormalities in patients. Future work will evaluate more spatial assessments and include results from clinical ophthalmologist assessments of the parametric map results compared to all other collected clinical images (e.g., fluorescein angiography, OCT, OCT-angiography, and color fundus imaging).

Several obstacles, including patient eye motion, limited SLO bit-depth (8-bit), and larger vessel signal saturation, had to be overcome to make it possible to achieve high-fidelity fits of FVA data with the modified AATH model. It is likely that these obstacles have obstructed the adoption of tracer kinetic modeling in past retinal FVA data analyses. The observed statistically significant differences in E between control, DMnoDR, and mild NPDR subjects highlight the unmatched sensitivity of the proposed approach to detecting subtle changes in retinal vascular health. It should be noted also that while there was no statistically significant difference between the Es of the DMnoDR and mild NPDR groups, the mean mild NPDR E was higher than the mean of the DMnoDR. Elucidating the statistical significance of the NPDR versus DMnoDR E differences will require a larger sample size of mild NPDR subjects; however, this does not detract from the impact of the present work since this is the first observation of differences in vascular health between DMnoDR and controls.

In summary, this work presents the first demonstration of a method to map vascular permeability in the retina of human subjects. In early results from a larger clinical study, it was shown that measures of E were significantly higher in DMnoDR compared with control subjects. This may have significant clinical implications considering there is currently no other retinal imaging device capable of detecting the subtle differences in retinal vascular permeability in patients with diabetes and no signs of diabetic retinopathy and control subjects. Such findings may help elucidate which DMnoDR patients are more likely to progress to NPDR in the future (this is an aim of the larger clinical study).

Footnotes and Disclosures

Originally received: July 17, 2024.
Final revision: October 4, 2024.
Accepted: October 21, 2024.
Available online: October 26, 2024. Manuscript no. XOPS-D-24-00242.

[1] Department of Biomedical Engineering, Illinois Institute of Technology, Chicago, Illinois.

[2] Department of Ophthalmology, Feinberg School of Medicine, Northwestern University, Chicago, Illinois.

[3] Department of Ophthalmology and Visual Sciences, Illinois Eye and Ear Infirmary, University of Illinois at Chicago, Chicago.

[4] Department of Biomedical Engineering, Stevens Institute of Technology, Hoboken, New Jersey.

Sarah R. Vavrek, Nicholas Konopek, Bou-Ghanem, Amani A. Fawzi, William F. Mieler, Kenneth M. Tichauer, and Jennifer J. Kang-Mieler presented "A one-year follow-up of retinal vascular permeability extracted from fluorescein videoangiographies (FVA) of diabetic subjects with no diabetic retinopathy (DMnoDR)." *Investigative Ophthalmology & Visual Science* 2024;65(7):1753−1753.

Disclosures:

All authors have completed and submitted the ICMJE disclosures form.

The authors made the following disclosures:

A.A.F.: Grants − NIH, Boehringer Ingelheim; Consulting fees − Genentech/Roche, Inc., Regenxbio, Boehringer Ingelheim, 3Helix.

E.K.N.: Grants − NIH 5U54AR079795-03 (paid to institution).

Supported by the National Institute of Health grant R01EY032222. S.R.V. acknowledges additional support from the Achievement Rewards for College Scientists "Pat and John Anderson" Scholarship.

HUMAN SUBJECTS: Human subjects were included in this study. All procedures were carried out with approval from Institutional Review Boards at Northwestern University and the University of Illinois Chicago, who reviewed clinical procedures based on the principles embodied in the Declaration of Helsinki. The study was conducted at the Department of Ophthalmology and Visual Sciences at the University of Illinois Chicago and the Department of Ophthalmology at Northwestern University, with the understanding and written consent of each subject.

No animal subjects were used in this study.

Author Contributions:

Conception and design: Fawzi, Mieler, Tichauer, Kang-Mieler

Data collection: Vavrek, Nalbant, Konopek, Decker, Fawzi, Mieler, Tichauer, Kang-Mieler

Analysis and interpretation: Vavrek, Tichauer

Obtained funding: N/A

Overall responsibility: Vavrek, Fawzi, Mieler, Tichauer, Kang-Mieler

Abbreviations and Acronyms:
AATH = adiabatic approximation to the tissue homogeneity; **ANOVA** = analysis of variance; **AVIs** = Audio Video Interleaves; **BMI** = body mass index; **DMnoDR** = diabetes mellitus no diabetic retinopathy; **DR** = diabetic retinopathy; **DTKM** = dynamic tracer kinetic model; **FVA** = fluorescein videoangiography; **IOP** = intraocular pressure; **NPDR** = nonproliferative diabetic retinopathy; **PI** = permeability index; **PS** = permeability-surface area product; **ROI** = region of interest; **SLO** = scanning laser ophthalmoscope.

Keywords:
Retinal vascular permeability, Diabetic retinopathy, Biomarker, Fluorescein videoangiography.

Correspondence:
Jennifer J. Kang-Mieler, PhD, Department of Biomedical Engineering, Stevens Institute of Technology, 1 Castle Point Terrace, Hoboken, NJ 07030. E-mail: jkangmie@stevens.edu.

References

1. CDC. *Keep an Eye on Your Vision Health*. Centers for Disease Control and Prevention; 2020. https://www.cdc.gov/visionhealth/resources/features/keep-eye-on-vision-health.html. Accessed October 16, 2021.
2. Cunha-Vaz JG, Shakib M, Ashton N. Studies on the permeability of the blood-retinal barrier. I. On the existence, development, and site of a blood-retinal barrier. *Br J Ophthalmol*. 1966;50:441−453.
3. Schmetterer L, Wolzt M. Ocular blood flow and associated functional deviations in diabetic retinopathy. *Diabetologia*. 1999;42:387−405.
4. Beltramo E, Porta M. Pericyte loss in diabetic retinopathy: mechanisms and consequences. *Curr Med Chem*. 2013;20:3218−3225.
5. Porta M. Endothelium: the main actor in the remodelling of the retinal microvasculature in diabetes. *Diabetologia*. 1996;39:739−744.
6. Schalkwijk CG, Stehouwer CDA. Vascular complications in diabetes mellitus: the role of endothelial dysfunction. *Clin Sci*. 2005;109:143−159.
7. Xu Q, Qaum T, Adamis AP. Sensitive blood-retinal barrier breakdown quantitation using Evans blue. *Invest Ophthalmol Vis Sci*. 2001;42:789−794.
8. Chakrabarti S, Cukiernik M, Hileeto D, et al. Role of vasoactive factors in the pathogenesis of early changes in diabetic retinopathy. *Diabetes Metabol Res Rev*. 2000;16:393−407.
9. Antonetti DA, Silva PS, Stitt AW. Current understanding of the molecular and cellular pathology of diabetic retinopathy. *Nat Rev Endocrinol*. 2021;17:195−206.
10. Russ PK, Gaylord GM, Haselton FR. Retinal vascular permeability determined by dual-tracer fluorescence angiography. *Ann Biomed Eng*. 2001;29:638−647.
11. Choi WJ. *Measurement of Retinal Vascular Permeability in a Rat Model Using Spectroscopic Optical Coherence*

Tomography. Thesis: Massachusetts Institute of Technology; 2011. https://dspace.mit.edu/handle/1721.1/68441. Accessed October 19, 2022.
12. Allen CL, Malhi NK, Whatmore JL, et al. Non-invasive measurement of retinal permeability in a diabetic rat model. *Microcirculation*. 2020;27:e12623.
13. Antonetti DA, Barber AJ, Khin S, et al. Vascular permeability in experimental diabetes is associated with reduced endothelial occludin content: vascular endothelial growth factor decreases occludin in retinal endothelial cells. Penn State Retina Research Group. *Diabetes*. 1998;47:1953−1959.
14. Nakajima M, Cooney MJ, Tu AH, et al. Normalization of retinal vascular permeability in experimental diabetes with genistein. *Invest Ophthalmol Vis Sci*. 2001;42:2110−2114.
15. Lee TY, Purdie TG, Stewart E. CT imaging of angiogenesis. *Q J Nucl Med*. 2003;47:171−187.
16. Larsson HB, Stubgaard M, Frederiksen JL, et al. Quantitation of blood-brain barrier defect by magnetic resonance imaging and gadolinium-DTPA in patients with multiple sclerosis and brain tumors. *Magn Reson Med*. 1990;16:117−131.
17. Tofts PS, Kermode AG. Measurement of the blood-brain barrier permeability and leakage space using dynamic MR imaging. 1. Fundamental concepts. *Magn Reson Med*. 1991;17:357−367.
18. Brix G, Semmler W, Port R, et al. Pharmacokinetic parameters in CNS Gd-DTPA enhanced MR imaging. *J Comput Assist Tomogr*. 1991;15:621−628.
19. Rosen RB, Andrade Romo JS, Krawitz BD, et al. Earliest evidence of preclinical diabetic retinopathy revealed using optical coherence tomography angiography perfused capillary density. *Am J Ophthalmol*. 2019;203:103−115.
20. Palochak CMA, Lee HE, Song J, et al. Retinal blood velocity and flow in early diabetes and diabetic retinopathy using adaptive optics scanning laser ophthalmoscopy. *J Clin Med*. 2019;8:1165.
21. Zhang B, Chou Y, Zhao X, et al. Early detection of microvascular impairments with optical coherence tomography angiography in diabetic patients without clinical retinopathy: a meta-analysis. *Am J Ophthalmol*. 2021;222:226−237.
22. Mehta NS, Lee JG, Gupta L, et al. Correlation of OCT angiography vessel densities and the early treatment diabetic retinopathy study grading scale. *Oph Retina*. 2021;5:714−715.
23. Waheed NK, Rosen RB, Jia Y, et al. Optical coherence tomography angiography in diabetic retinopathy. *Prog Retin Eye Res*. 2023;97:101206.
24. Spaide RF, Fujimoto JG, Waheed NK, et al. Optical coherence tomography angiography. *Prog Retin Eye Res*. 2018;64:1−55.
25. Meier P, Zierler KL. On the theory of the indicator-dilution method for measurement of blood flow and volume. *J Appl Physiol*. 1954;6:731−744.
26. St Lawrence KS, Lee TY. An adiabatic approximation to the tissue homogeneity model for water exchange in the brain: I. Theoretical derivation. *J Cereb Blood Flow Metab*. 1998;18:1365−1377.
27. Johnson J, Wilson T. A model for capillary exchange. *Am J Physiol*. 1966;210:1299−1303.
28. Tichauer KM, Osswald CR, Dosmar E, et al. Estimating retinal vascular permeability using the adiabatic approximation to the tissue homogeneity model with fluorescein videoangiography. *Biophotonics*. 2015;9531:47−53. SPIE.
29. Tichauer KM, Guthrie M, Hones L, et al. Quantitative retinal blood flow mapping from fluorescein videoangiography using tracer kinetic modeling. *Opt Lett*. 2015;40:2169−2172.
30. Vavrek SR, Nalbant EK, Konopek NJ, et al. Fluorescein videoangiography data analysis protocol for mapping retinal vascular permeability in humans. In: *Ophthalmic Technologies XXXIII*. Vol 12360. San Francisco, CA: SPIE; 2023:106−112.
31. O'Connor NJ, Bartsch DU, Freeman WJ, et al. Fluorescent infrared scanning-laser ophthalmoscope for three-dimensional visualization: automatic random-eye-motion correction and deconvolution. *Appl Opt*. 1998;37:2021−2033.
32. Campbell R. notBoxPlot. https://github.com/raacampbell/notBoxPlot; 2022. Accessed December 25, 2022.
33. Chan A, Duker JS, Ko TH, et al. Normal macular thickness measurements in healthy eyes using stratus optical coherence tomography. *Arch Ophthalmol*. 2006;124:193−198.
34. Zeimer RC, Blair NP, Cunha-Vaz JG. Vitreous fluorophotometry for clinical research. I. Description and evaluation of a new fluorophotometer. *Arch Ophthalmol*. 1983;101:1753−1756.
35. Zeimer RC, Blair NP, Cunha-Vaz JG. Vitreous fluorophotometry for clinical research. II. Method of data acquisition and processing. *Arch Ophthalmol*. 1983;101:1757−1761.
36. Cunha-Vaz JG, Gray JR, Zeimer RC, et al. Characterization of the early stages of diabetic retinopathy by vitreous fluorophotometry. *Diabetes*. 1985;34:53−59.
37. Chahal P, Fallon TJ, Jennings SJ, et al. Vitreous fluorophotometry in patients with no or minimal diabetic retinopathy. *Diabetes Care*. 1986;9:134−139.
38. Roy MS, Bonner RF, Bungay PM, et al. Posterior vitreous fluorophotometry in normal subjects. *Arch Ophthalmol*. 1986;104:1004−1008.
39. Patel V, Rassam S, Newsom R, et al. Retinal blood flow in diabetic retinopathy. *BMJ*. 1992;305:678−683.
40. Feke GT, Tagawa H, Deupree DM, et al. Blood flow in the normal human retina. *Invest Ophthalmol Vis Sci*. 1989;30:58−65.
41. Nagahara M, Tamaki Y, Tomidokoro A, Araie M. In vivo measurement of blood velocity in human major retinal vessels using the laser speckle method. *Invest Ophthalmol Vis Sci*. 2011;52:87.
42. Ahmed J, Pulfer MK, Linsenmeier RA. Measurement of blood flow through the retinal circulation of the cat during normoxia and hypoxemia using fluorescent microspheres. *Microvasc Res*. 2001;62:143−153.
43. Seddone S, Ermini L, Policastro P, et al. Evidence that large vessels do affect near infrared spectroscopy. *Sci Rep*. 2022;12:2155.
44. Calfon MA, Vinegoni C, Ntziachristos V, Jaffer FA. Intravascular near-infrared fluorescence molecular imaging of atherosclerosis: toward coronary arterial visualization of biologically high-risk plaques. *JBO*. 2010;15:011107.
45. Firbank M, Okada E, Delpy DT. Investigation of the effect of discrete absorbers upon the measurement of blood volume with near-infrared spectroscopy. *Phys Med Biol*. 1997;42:465−477.
46. Jacques SL. Optical properties of biological tissues: a review. *Phys Med Biol*. 2013;58:R37.